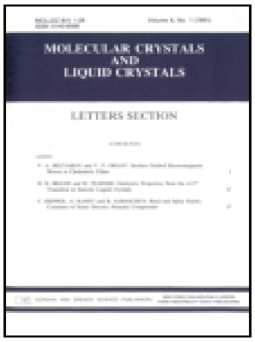

Taylor & Francis
Taylor & Francis Group

Molecular Crystals and Liquid Crystals

ISSN: 1542-1406 (Print) 1563-5287 (Online) Journal homepage: http://www.tandfonline.com/loi/gmcl20

Graphene oxide modified with aminoazobenzol group stabilized blue phase liquid crystals

Zongcheng Miao, Dong Wang, Hong Gao, Xiaomei Wang, Jianming Gu & Huiying Hu

To cite this article: Zongcheng Miao, Dong Wang, Hong Gao, Xiaomei Wang, Jianming Gu & Huiying Hu (2016) Graphene oxide modified with aminoazobenzol group stabilized blue phase liquid crystals, Molecular Crystals and Liquid Crystals, 634:1, 33-40, DOI: 10.1080/15421406.2016.1190141

To link to this article: http://dx.doi.org/10.1080/15421406.2016.1190141

MOLECULAR CRYSTALS AND LIQUID CRYSTALS
2016, VOL. 634, 33–40
http://dx.doi.org/10.1080/15421406.2016.1190141

Graphene oxide modified with aminoazobenzol group stabilized blue phase liquid crystals

Zongcheng Miao[a], Dong Wang[b], Hong Gao[c], Xiaomei Wang[b], Jianming Gu[d], and Huiying Hu[e]

[a]Xijing University, Xi'an, Shaanxi Province, PR China; [b]Department of Materials Physics and Chemistry, School of Materials Science and Engineering, University of Science and Technology Beijing, Beijing, PR China; [c]Division of Material Engineering, China Academy of Space Technology, Beijing, PR China; [d]Department of Adult Joint Reconstruction, Beijing Jishuitan Hospital, Beijing, PR China; [e]Department of Obsterics and Gynecology, Peking Union Medical College Hospital, Beijing, PR China

ABSTRACT
Liquid-crystalline blue phases are stable only for very narrow temperature range between the isotropic and the chiral nematic phase that severely hinders their applicability. Herein, aminoazobenzol group was chemically grafted onto graphene oxide (GO) via amidization reaction. Successful grafting of aminoazobenzol group was confirmed using X-ray photoelectron spectroscopy (XPS), Fourier transform infrared spectroscopy (FT-IR), UV-vis absorption spectra and Thermogravimetric analysis (TGA). The resultant aminoazobenzol group modified GO sheets which is reduced (GO-Az) were easily redispersed in common organic solvents. By doping different contents of GO-Az nanosheets could stabilize blue phase and increase the blue phase range. When doped with 0.5 wt% GO-Az, the mixtures show the wider range with 5.4°C than the range with 3.6°C of blue phase liquid crystals without GO-Az. Meanwhile, the phase sequence and the range of the aforementioned phases are reproducible upon heating and cooling, which shows that the blue phases doped with GO-Az nanosheets are thermodynamically stable.

KEYWORDS
Blue phase liquid crystals; graphene; wider temperature range

Introduction

Liquid-crystal nano science has attracted special attention in recent years due to the potential applications in developing new composite materials [1,2]. Combinations of liquid crystals (LCs) [3–5] and nanomaterials have currently sparked enormous interest from very fundamental studies on interactions of nanomaterials with LC phases to LC template syntheses of nanomaterials, to nanoparticles (NPs) as dopants for LCs used in electro-optic devices [6–10]. Doping nematic LCs with nanoparticles has lead to many promising LC electro-optical characteristics including low driving voltages, short response time, frequency modulation response, and memory effect [11–14].

Among currently available nanomaterials, graphene, has attracted immense attention for potential applications in electronic devices and nanocomposites since its successful isolation in 2004 [15]. Due to unique structure and outstanding properties, graphene, the

---

CONTACT Dong Wang ✉ wangdong@ustb.edu.cn Department of Materials Physics and Chemistry, School of Materials Science and Engineering, University of Science and Technology Beijing, Beijing, 100083, PR China
Color versions of one or more of the figures in the article can be found online at www.tandfonline.com/gmcl.

two-dimensional sp2-hybridized carbon, is currently, without any doubt, the most intensively studied material [16,17]. Graphene oxide (GO), one of the most important derivatives of graphene, is structurally similar to graphene. However, the surface of GO contains large numbers of hydrophilic functional groups, such as carbonyl, carboxyl, epoxy, and hydroxyl, which afforded GO with excellent processability, dispersibility; thus GO becomes a promising functional nano reinforcing material for various polymer and organic molecules to approach different advanced applications [18–22]. In current nanoscience, researchers have studied the optical manipulation in a LC/graphene nanostructure as well as applications of graphene in cholesteric and polymer-dispersed LCs [23–25].

Liquid-crystalline blue phases (BPs) have sparked an enormous interest due to their exotic optical properties [26,27]. However, blue phases appear within a narrow temperature range, due to the free-energy cost of disclination [28]. Suspensions of NPs in BPs were believed to replace part of the energetically costly disclination region with the particles' own volume [29]. This approach could enhance the stability of BPs. In this paper, the azobenzene grafted graphene nanosheets was designed and prepared, and the solubility of GO in solvent and LC was expected to increase. The GO-Az was dispersed in the BPLCs, and the interaction between BPLCs and GO-Az was investigated in detail.

Experimental

Graphite powder (320 mesh) was purchased from Sinopharm Chemical Reagent. Co., Ltd. Aminoazobenzol was purchased from Aladdin Reagent (Shanghai) Co., Ltd. The other reagents were purchased from Beijing Lan Yi Chemical Products Co., Ltd.

Preparation of GO nanosheets

GO was prepared using a modification of Hummers and Offeman's method [30–33]. In a typical reaction, 1 g graphite, 1 g $NaNO_3$, and 50 mL H_2SO_4 were stirred together in an ice bath. $KMnO_4$ (6 g) was slowly added while stirring, and the rate of addition was controlled to prevent the mixture temperature from exceeding 20°C. The mixture was then transferred to a 35°C water bath and stirred for about 0.5 hr, forming a thick paste. Subsequently, 50 mL de-ionized water was added gradually, causing an increase in temperature to 98°C. After 15 min, the mixture was further treated with 150 mL de-ionized water and 10 mL 30% H_2O_2 solution. The warm solution was then filtered and washed with de-ionized water until the pH was 7 and dried at 65°C under vacuum.

Preparation of Az-grafted graphene

In a typical experiment for the synthesis of the aminoazobenzol-grafted graphene, the dried GO sample (100 mg) was refluxed in thionyl chloride (40 mL) for 24 hr. The product was centrifuged (5000 rpm for 25 min), and the supernatant was decanted away. The remaining solid material was dried under vacuum for 3 hr. aminoazobenzol (0.6 g) in 50 mL THF was then added through a syringe to the thionyl chloride treated GO under stirring, followed by the addition of triethylamine (15 mL) in nitrogen atmosphere. After sonicated for 2 hr, the reaction mixture was vigorously stirred for 36 hr, leading to a dark suspension. Then the mixture was filtered with a Teflon-filter (0.2 mm), and washed with THF for 4 times, the remaining solid material (GO-Az) was dried under vacuum.

The BP-exhibiting LC material was a mixture comprising the following materials: P70 (97.0 wt%, Yongsheng Huatsing Liquid Crystal Co., Ltd, birefringence: $\Delta n = 0.156$, dielectric anisotropy: $\Delta\varepsilon = 33.6$ at 298 K), R5011 (3.0 wt%, Merck). The liquid-crystalline composites doped with different concentration of GO-Az nanosheets were prepared by dispersing the nanosheets into the BP-exhibiting LC material.

X-ray photoelectron spectroscopy (XPS) was performed on vacuum filtered films in a system equipped with a VG CLAMII electron analyzer and PSP twin anode source. Mg Ka (hm = 1253.6 eV) spectra were recorded at 10-eV pass energy and 2-mm slits, yielding an overall energy resolution of 0.85 eV. Samples were introduced via a load lock and measurement base pressure was better than 10^{-9} mbar. Fourier transform (FTIR) spectra were recorded on a NEXUS 670 spectrometer. Thermogravimetric analysis (TGA, Netzsch TG 209) was conducted in a nitrogen atmosphere from ambient temperature to 1000°C with a heating rate of 5°C/min. The initial phase assignments and corresponding transition temperatures for the final compounds were determined by using the thermal optical microscopy with a polarizing microscope (Olympus BX-51) equipped with a hot stage calibrated to an accuracy of ±0.1°C (Linkam LK-600PM).

Results and discussion

A typical procedure for preparing aminoazobenzol functionalized graphene nanosheets was presented in Fig. 1. The final GO-Az product can be easily redispersed in common organic solvents, such as THF, chloroform, and toluene under sonication.

Figure 2 shows XPS of GO before and after grafting with aminoazobenzol. While Fig. 2a shows only the carbon and oxygen peaks for GO, the corresponding XPS spectra for the purified GO-Az in Fig. 2b reveal the presence of carbon, oxygen, and nitrogen, arising from the aminoazobenzol and graphene sheets. Fig. 2c reproduces the high-resolution C1s spectra for GO, which exhibits the presence of C-C (284.6), C-O (286.5), and C=O (288.2) groups. Upon aminoazobenzol grafting (Fig. 2d), the intensities of the C-O and C=O peaks decreased dramatically due to the formation of amide linkages between the COOH groups of GO and aminoazobenzol. The presence of the amide linkages in GO-Az is also evidenced by the C=O and C-N peaks at 285.9 eV in Fig. 3d, though the contribution from some unreacted functional groups in the GO cannot be ruled out. While the amidation reaction between the

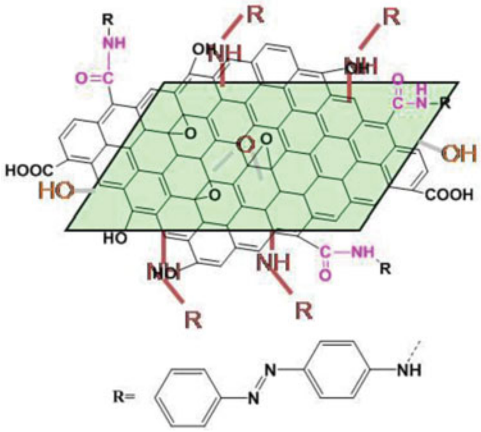

Figure 1. Synthesis route of aminoazobenzol group grafted on graphene nanoplatelets.

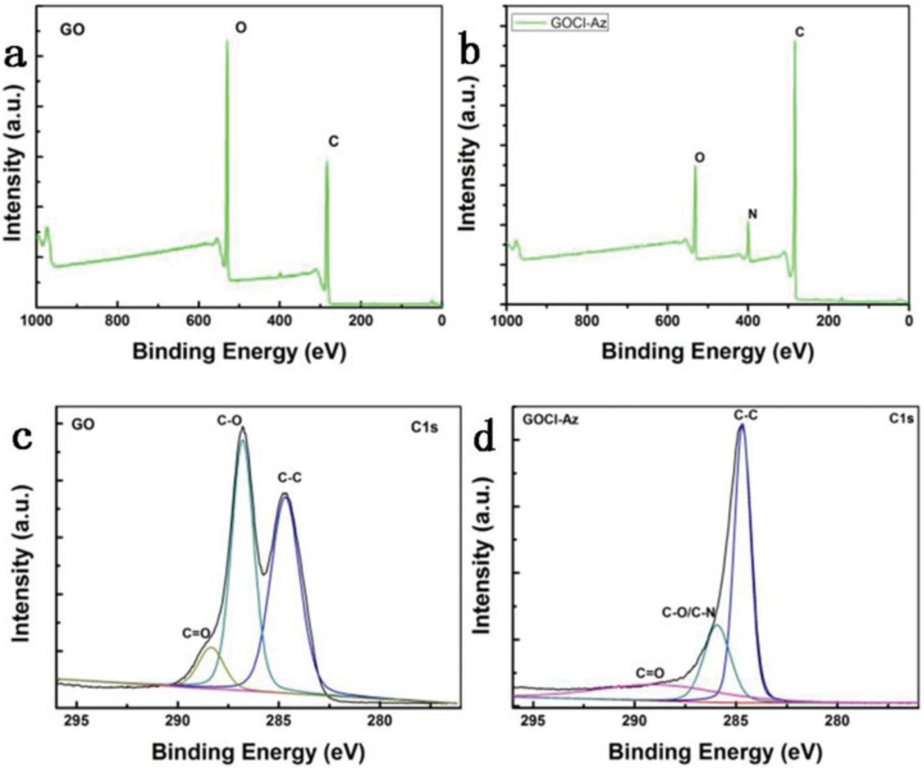

Figure 2. XPS spectra of GO and GO-Az (a, b) Survey spectra and (c, d) high-resolution C1s spectra.

acyl-chloride functionalized GO and aminoazobenzol significantly reduced the COOH component of GO, the significant decrease of the C-O component in Fig. 2c suggests possible activation of the -OH groups of GO by thionyl chloride and subsequent grafting aminoazobenzol onto the activated -OH group of GO by the formation of C(O)-NH linkage (Fig. 2) [34].

FTIR spectra (in Fig. 3) gave further evidence on the GO and GO-Az. As shown in Fig. 3, the pure GO shows the peaks of OH (O-H stretching vibrations) at 3430 cm^{-1}, C=O (carboxylic acid and carbonyl moieties) at 1734 cm^{-1}, along with the broad band over 1000–1400 cm^{-1} arising from the C-O (1075 cm^{-1}) stretching vibrations [34]. For the GO-Az (in Fig. 3), the bands at 1734 and 1627 cm^{-1} were disappeared, and the bands at 2990

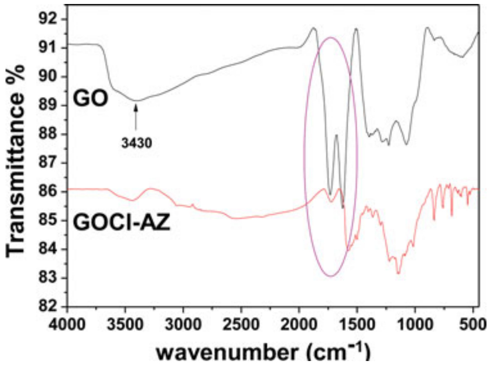

Figure 3. FTIR spectra of GO and GO-Az.

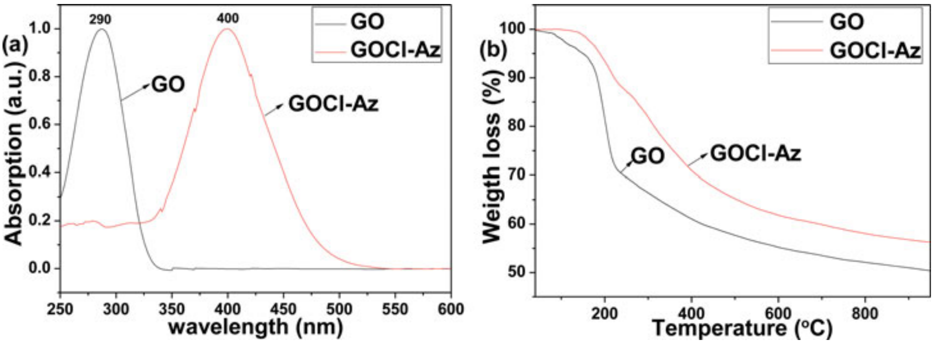

Figure 4. (a) UV-vis spectra of GO and GO-Az; (b) TGA curves of GO and GO-Az.

and 1550 cm^{-1} can be attributed to the C-N stretching of the amino groups, confirming the formation of covalent bonding between graphene and aminoazobenzol groups.

Figure 4a shows the normalized UV absorption spectra of pure GO and GO-Az in N,N-dimethylformamide (DMF) solution. A strong absorption band at 290 nm attributable to the π-π^* transition was seen for pure GO. Upon grafting aminoazobenzol onto graphene in GO-Az, the band red-shifted to about 400 nm. These results indicate that there exists a strong interaction between aminoazobenzol group and graphene in GO-Az.

Figure 4b shows thermo-gravimetric curves from the GO and the GO-Az sample. GO is not thermally stable, and mass weight loss started below 100°C and was rapid at 150°C. The results attributed mass weight loss in the early stage to the pyrolysis of labile oxygen-containing groups such as –OH, COOH etc [35]. The rapid weight loss (25 wt%) in the temperature range of 150°C–200°C is attributed to the removal of oxygen containing functional groups from the GO surface. It would improve the thermal stability of GO with the decrease in defect density, which is consistent with the thermal behavior of aminoazobenzol group grafted GO. Meanwhile, a higher weight loss (15 wt%) is observed between 300°C and 500°C in GO-Az, which is corroborated to the degradation of aminoazobenzol group attached to the GO.

All the results suggest that the aminoazobenzol molecules have been successfully modified onto GO. Then the blue phase liquid-crystal were doped with different contents of GO-Az and GO, separately, and the BP-exhibiting LC material was a mixture comprising the following materials: P70 (97.0 wt%), R5011 (3.0 wt%). After ultrasonic dispersion and solvent evaporation, the blends were placed into planar treated cells by capillary action, and the cell gap was maintained at 25 μm by spacer. The compositions and the weight ratios of the five studied samples are listed in Table 1. The blue phase ranges of the samples were shown in Table 1 while cooling the samples at a rate of 0.5°C/min.

As shown in Table 1 and Fig. 5(a), when doped without GO-Az, the blue phase range is 3.6°C. However, when doped with GO-Az ranging from 0.1 to 0.5 wt%, the mixtures show

Table 1. Chemical compositions and blue phase range of samples 1–5.

Samples	Nanomaterials/wt%	BPLC/wt%	Temp. range/°C
1	0.0	71.4–67.8	3.6
2	0.1	71.8–66.9	4.9
3	0.3	72.2–67.2	5.0
4	0.5	72.7–67.3	5.4
5	0.7	71.9–67.8	4.1

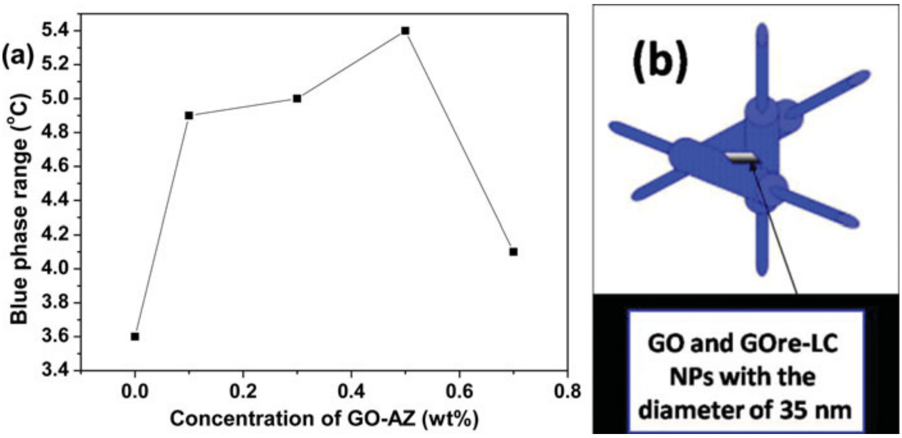

Figure 5. (a) Effect of the concentration of GO-Az on the blue phase range of liquid-crystalline composites; (b) The disclination lattices of BPI stabilized by the GO-Az NPs.

an increasing BP range with the widest to 5.4°C, whereas further addition of the nanosheets suppresses the range. The stability of BPs depends on a well-arranged double-twisted alignment and a stable defect. A possible mechanism for the BPI stabilized by GO-Az nanosheets can be depicted as in Fig. 5(b). Theoretical simulation has found that nanoparticles doped in BPs will most likely be trapped in the disclination lines as a result of elastic interactions [30]. The initially freely moving GO-Az nanosheets became trapped once they met a disclination line, and the volume and the free energy around the disclinations were consequently reduce. The volume and the free energy around the disclinations could be continuously suppressed with increasing the concentration of GO-Az nanosheets, but the cubic structures of BP would be disordered after the critical concentration had been reached. The above viewpoint may be a possible interpretation for the effect of the concentration of GO-Az nanosheets on the BP range of the composites.

Figure 6 shows the typical textures of BP stabilized by 0.5 wt% GO-Az nanosheets during the cooling process. The black texture is GO-Az nanosheets. Upon cooling gradually from the isotropic phase a platelet texture, which is a peculiar optical texture of the BP I phase, was observed in the temperature range 72.7°C–67.3°C (Fig. 6a, b, and c). More importantly, the phase sequence and the range of the aforementioned phases are reproducible upon heating and cooling. Hence, the blue phases of P70 and GO-Az nanosheets mixture are thermodynamically stable.

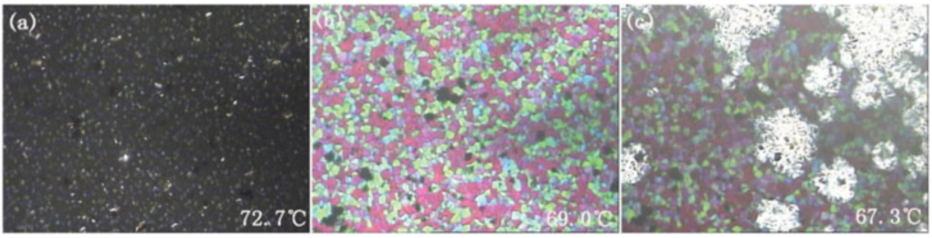

Figure 6. POM photos of the natural textures of BP stabilized by 0.5 wt% GO-Az nanosheets on cooling.

Conclusions

In conclusion, we have successfully modified the azobenzene molecules onto GO. Besides, the effect of the concentration of GO-Az nanosheets on the blue phase stability range of P70 was investigated. It was found that a minute concentration of graphene was sufficient to extent the blue phase range, affecting mostly the ordered BPI. The temperature range of BPLC could be extended to about 5.4°C by the dispersion of 0.5 wt% of GO-Az nanosheets, which may result from that the volume and the free energy around the disclinations were suppressed by introducing the GO-Az nanosheets. We hope that our observations are expected to meaningful for developing the BP composites.

Acknowledgments

This work was supported by the National Key Basic Research Program of China (No. 2014CB931804), Natural Science Basic Research Plan in Shaanxi Province of China (No. 2013JQ8043).

References

[1] Qi, H., & Hegmann, T. (2008). *J. Mater. Chem.*, *18*, 3288–3294.
[2] Bisoyi, H. K., & Kumar, S. (2011). *Chem. Soc. Rev.*, *40*, 306–319.
[3] Yu, H., & Ikeda, T. (2011). *Adv. Mater.*, *23*, 2149–2180.
[4] White, T. J., Bricker, R. L., Natarajan, L. V., Tabiryan N. V., Green L., Li Q., & Bunning T.J. (2009). *Adv. Funct. Mater.*, *19*, 3484–3488.
[5] Wang, H. H., Wang, L., Xie, H., Li, C. Y., Guo, S. M., Wang, M., Zou, C., Yang, D. K., & Yang, H. (2015). *RSC Adv.*, *5*, 33489–33495.
[6] Dong, X., Long, Q., Wang, J., Chan-Park, M. B., Huang, Y., & Chen, P. (2011). *Nanoscale*, *3*, 5156–5160.
[7] Dong, X., Xing, G., Chan-Park, M. B., Shi, W., Xiao, N., Wang, J., & Chen, P. (2011). *Carbon*, *49*, 5071–5078.
[8] Dong X., Long, Q., Wei, A., Zhang, W., Li, L. J., Chen, P., & Huang, W. (2012). *Carbon*, *50*, 1517–1522.
[9] Dong, X., Huang, W., & Chen, P. (2011). *Nano. Res. Lett.*, *6*, 1–6.
[10] Stamatoiu, O., Mirzaei, J., Feng, X., & Hegmann, T. (2012). *Top. Curr. Chem.*, *318*, 331–393.
[11] Kaur, S., Singh, S. P., Biradar, A. M., Choudhary, A., & Sreenivas, K. (2007). *Appl. Phys. Lett.*, *91*, 023120.
[12] Li, B. F., Huang, H., Ding, X. K., Li, W. B., Yin, Y. H., Wang, L. P., Cao, H., & Yang, H. (2008). *Liq. Cryst.*, *35*, 49–54.
[13] Shiraishi, Y., & Toshima, N. (2002). *Appl. Phys. Lett.*, *81*, 2845–2847.
[14] Lee, W., Wang, C. Y., & Shih, Y. C. (2004). *Appl. Phys. Lett.*, *85*, 513–515.
[15] Twombly, C. W., Evansand, J. S., & Smalyukh, I. (2013). *Opt. Express.*, *21*, 1324–1334.
[16] Geim, A. K. (2009). *Science*, *324*, 1530–1534.
[17] Geim, A. K., & Novoselov, K. S. (2007). *Nat Mater*, *6*, 183–191.
[18] Marcano, D.C., Kosynkin, D.V., Berlin, J.M., Sinitskii, A., Sun, Z.Z., Slesarev, A., Alemany, L.B., Lu W., & Tour, J.M. (2010). *ACS Nano*, *4*, 4806–4814.
[19] Longun, J., & Iroh, J.O. (2012). *Carbon*, *50*, 1823–1832.
[20] Szabó, T., Berkesi, O., & Dékány, I. (2005). *Carbon*, *43*, 3186–3189.
[21] Ramanathan, T., Abdala, A. A., Stankovich, S., Dikin D. A., Herrara-Alonso, M., Piner, R. D., Adamson, D. H., Schniepp, H. C., Chen X., Ruoff, R. S., Nguyen, S. T., Aksay, I. A., Prud'homme, R. K., & Brinson, L. C. (2008). *Nat. Nanotechnol.*, *3*, 327–331.
[22] Stankovich, S., Dikin, D. A., Dommett, G. H. B., Kohlhaas, K. M., Zimney, E. J., Stach, E. A., Piner, R. D., Nguyen, S. T., & Ruoff, R. S. (2006). *Nature*, *442*, 282–286.
[23] Xu, Z., & Gao, C. (2011). *Nature Commun*, *2*, 571.
[24] Kim, B. K., Jang, M.W., Park, H. C., Jeong, H. M., & Kim, E. Y. (2012). *J. Polym. Sci. Part A: Polym. Chem.*, *50*, 1418–1423.

[25] Bian, Z. Y., Li, K. X., Huang, W., Cao, H., & Yang, H. (2007). *Appl. Phys. Lett.*, *91*, 201908.

[26] Cao, W., Munoz, A., Palffy-Muhoray, P., & Taheri, B. (2002). *Nat. Mater.*, *1*, 111–113.

[27] Yan, J., Rao, L., Jiao, M., Cheng, H.C., & Wu, S.T. (2011). *J. Mater. Chem.*, *21*, 7870–7877.

[28] Ravnik, M., Alexander, G. P., Yeomans, J. M., & Zumer, S. (2010). *Faraday Discuss.*, *144*, 159–169.

[29] Rozic, B., Tzitzios, V., Karatairi, E., Tkalec, U., Nounesis, G., Kutnjak, Z., Gordoyiannis, G., Rosso, R., Virga, E. G., Musevic, I., & Kralj, S. (2011). *Eur. Phys. J. E*, *34*, 17.

[30] Stankovich, S., Piner, R. D., Chen, X. Q., Wu, N. Q., Nguyen, S. T., & Ruoff, R. S. (2006). *J. Mater. Chem.*, *16*, 155–158.

[31] Hummers, W. S., & Offeman, R. E. (1958). *J. Am. Chem. Soc.*, *80*, 1339.

[32] Gilje, S., Han, S., Wang, M., Wang, K. L., & Kaner, R. B. (2007). *Nano Lett.*, *7*, 3394–3398.

[33] Kovtyukhova, N. I., Ollivier, P. J., Martin, B. R., Mallouk, T. E., & Chizhik, S. A. (1999). *Chem. Mater.*, *11*, 771–778.

[34] Paredes, J.I., Villar-Rodil, S., Martinez-Alonso, A., & TascO´n, J. M. D. (2008). *Langmuir*, *24*, 10560–10564.

[35] Stankovich, S., Dikin, D. A., Piner, R. D., Kohlhaas, K. A., Kleinhammes, A., Jia, Y. Y., Wu, Y., Nguyen, S.T., & Ruoff, R.S. (2007). *Carbon*, *45*, 1558–1565.